



## Original Article



# Evaluation of Ophiolite Complex Impact and Pollution Indices of Groundwater Resources in Jovein Area (NE Iran)

Raheleh Hatifi<sup>1\*</sup>, Morteza Razmara Farzaghi<sup>2</sup>, Seyed Mohammad Zamanzadeh<sup>3</sup><sup>1</sup>Department of Environmental Geology, Research institute of Applied Science, ACECR, Tehran, Iran<sup>2</sup>Science Faculty, Department of Geology, Ferdowsi University, Mashhad, Iran<sup>3</sup>Department of Natural Geography, Faculty of Geology, University of Tehran, Tehran, Iran**Article history:**

Received: July 2, 2024

Revised: September 16, 2024

Accepted: October 1, 2024

ePublished: April 20, 2025

**\*Corresponding author:**

Raheleh Hatifi

Email: [hatefi@rias.ac.ir](mailto:hatefi@rias.ac.ir)**Abstract****Background:** Potential ore deposits and mining activities can cause soil and groundwater pollution with heavy metals, posing risks to human health. This study aimed to identify heavy metal sources, their transfer patterns, and contamination levels in the Jovein aquifer (NW Sabzevar, Iran).**Methods:** The groundwater samples were analyzed using inductively coupled plasma mass spectroscopy (ICP-MS). Pollution indices, including the heavy metal pollution index (HPI) and heavy metal evaluation index (HEI), were calculated. Statistical analyses such as principal component analysis (PCA) and cluster analysis (CA) were applied, and results were mapped using ArcGIS software.**Results:** The average element concentrations followed the order: Boron (B) > chromium (Cr) > barium (Ba) > vanadium (V) > arsenic (As) > aluminum (Al) > lithium (Li) > selenium (Se) > molybdenum (Mo) > copper (Cu) > zinc (Zn) > uranium (U) > tungsten (W) > antimony (Sb). PCA showed Cr and nickel (Ni) originated from weathering of chromite ores and ultramafic rocks, while As and Cu were linked to sulfide mineralization. Although HPI levels were elevated, they remained below critical thresholds. CA grouped samples into two clusters: one with Ni, Cr, and Cu, and the other with As and Sb.**Conclusion:** Geogenic processes are the main contributors to groundwater contamination, while mining activities have minimal influence in the Jovein aquifer. Overall, the assessment reveals poor groundwater quality due to heavy metal pollution.**Keywords:** Ophiolite complex, Pollution and evaluation indices, Statistical analysis, Jovein aquifer

**Please cite this article as follows:** Hatifi R, Razmara Farzaghi M, Zamanzadeh SM. Evaluation of ophiolite complex impact and pollution indices of groundwater resources in Jovein area (NE Iran). J Adv Environ Health Res. 2025; 13(2):121-128. doi:10.34172/jaehr.1389

**Introduction**

Groundwater is among the most vital and readily available resources for both irrigation and drinking water purposes.<sup>1,2</sup> Its quality significantly impacts human health, aquatic organisms, industry, and agriculture.<sup>3,4</sup> Groundwater pollution caused by heavy metals poses a major environmental challenge due to their toxic effects, even at low concentrations,<sup>5</sup> and their bioaccumulation in the food chain.<sup>6,7</sup> Pollution and insufficient recharge are major parameters driving the deterioration of groundwater quality.<sup>8</sup> The geochemical behavior of groundwater changes over time due to both natural (geogenic) and human-made factors, including weathering, lithology, evaporation, ion exchange, recharge sources, vegetation, precipitation, fertilizers, industrialization, and urbanization.<sup>9</sup> The Earth's crust serves as a geogenic source of heavy metals in groundwater, often attributed to the dissolution of natural minerals and materials within

it.<sup>10</sup> Moreover, ultramafic and mafic rocks contribute to heavy metal enrichment in ecosystems, exacerbating environmental degradation.<sup>11</sup> Serpentine soils, known for their low stability, also contain various heavy metals.<sup>12</sup> The management of groundwater quality presents noticeable challenges. Continuous monitoring is essential to mitigate the impact of polluted groundwater on various uses, such as domestic, hygiene, industrial, and agricultural purposes.<sup>13</sup> However, monitoring alone cannot provide a comprehensive understanding due to limited sample sizes and the complexity of multiple parameters. To address this, contamination indices serve as valuable tools for simplifying data, documenting findings, and mapping groundwater pollution status by integrating the effects of numerous parameters in the study area.<sup>14</sup> Numerous studies have investigated heavy metal pollution in water resources and developed various water quality indices.<sup>15,16</sup> These indices are crucial for evaluating water quality<sup>17</sup> and



include the heavy metal evaluation index (HEI), the degree of contamination ( $C_d$ ), and the heavy metal pollution index (HPI).<sup>18</sup> These tools are integral to planning, managing, and decision-making in water systems and have been widely used to assess groundwater pollution and health risks.<sup>6</sup> Statistical techniques, such as multivariate analysis, help identify the sources of groundwater pollution by reducing data complexity and clustering samples based on correlations between parameters.<sup>19</sup> The Jovein aquifer is a vital water source for both agriculture and drinking in the region, serving as the sole clean and relatively unpolluted water resource. The objective of this study was to assess the impact of the ophiolite complex and heavy metals on groundwater quality in the Jovein region. The hydrogeochemical characteristics, pollution sources, and processes affecting groundwater chemistry were investigated to evaluate the influence of heavy metals from various sources. This objective was accomplished through an integrated approach that combined pollution indices (such as HPI, HEI, and  $C_d$ ) with Multivariate Statistical Analysis, providing a thorough evaluation of the contamination status.

## Material and Methods

### Geology

The area studied is situated between 56° 45′–57° 50′ East longitudes and 36° 20′–36° 50′ North latitudes in the northwestern part of the Sabzevar region (NE Iran). It features dramatic topography, characterized by a plain that expands around mountainous areas. The Jovein aquifer lies downstream of the Sabzevar ophiolite complex. The Sabzevar ophiolite, situated in NE Iran, is part of the Mesozoic ophiolite belt. This complex spans approximately 10–30 km in width and 150 km in length.<sup>20</sup> The southern part of the area is covered by mountainous and irregular topography, while the northern part comprises low-lying hills. Rivers, serving as the primary recharge source for the Jovein aquifer, flow northward and eventually converge into the Jovein Kal Shor river. The depth of the aquifer varies significantly, ranging from approximately 200 meters in some areas to 6.5 meters near the outlet. Groundwater flow predominantly moves from the western side toward the Kal Shor river in the north. The study area primarily consists of Miocene formations and alluvial plains. Most wells are located within the ophiolitic complex, and the alluvial deposits are believed to play a crucial role in the aquifer's formation and recharge (Figure S1). Groundwater serves as the principal resource for agricultural activities and drinking water in this region.

### Hydro-Geological Setting

The main stratigraphic units in the area studied range from Precambrian to Quaternary formations. The Late Cretaceous ophiolite forms part of the Sabzevar ophiolite belt, which comprises peridotites (harzburgite, lherzolite, dunite) with podiform chromitite, layered gabbros, a

sheeted dike complex (diabasic and microgabbroic dikes), basaltic and andesitic rocks, and volcano-sedimentary deposits. The complex is covered by Upper Cretaceous to Paleocene volcanic rocks, which are linked to volcanoclastic sediments, pelagic limestone, and radiolarian chert.<sup>20</sup> Ophiolitic rocks are primarily composed of mafic and ultramafic rocks, exhibiting varying levels of serpentinization. Groundwater interacting with ophiolitic rocks and serpentinite is typically characterized as Mg-HCO<sub>3</sub> water,<sup>21</sup> often containing high contents of Cr and Ni.<sup>22</sup> The geology of the study region includes a thick stratigraphic sequence, beginning with Precambrian formations, followed by ophiolitic complexes, and capped by recent alluviums. The ophiolitic complex, from base to top, comprises peridotites, ultramafic cumulate rocks, mafic rocks, diabase dikes, pillowed and massive lava flows, and pyroclastic rocks (Figure S1). To the south, the ophiolitic complex (upper Cretaceous) is fault-bounded against Triassic flysch deposits and minor Cretaceous mélange. The area is overlain by Eocene sedimentary-volcanic and volcanic rocks. To the north, it is unconformably overlain by Neogene formations, including schists, phyllites, altered rhyolitic rocks, limestones, shales, sandstones, and marls. The main factors affecting groundwater quality in the study area are the ophiolitic complexes, Neogene formations, and Quaternary soils. Water quality varies based on the geological formations and sediments that make up the aquifer.

Groundwater sampling was carried out at 22 wells to evaluate water quality parameters and characterize the water chemistry in the study area. The locations of the sampling sites are shown in Figure S1. Parameters including pH, temperature, conductivity, and dissolved oxygen (DO) were measured in the field using a multi-parameter device. Water samples were collected in two 250 mL polyethylene containers, which were rinsed three times with water from the same source before sampling. To prevent precipitation on the container walls, nitric acid was used to acidify one set of samples. The second set of non-acidified samples was refrigerated at 4 °C upon arrival at the laboratory for preservation.

All analyses were performed at the Laboratory of the Regional Water Company (Khorasan Razavi) for anions, including Cl<sup>-</sup>, SO<sub>4</sub><sup>-2</sup>, CO<sub>3</sub><sup>-2</sup> and HCO<sub>3</sub><sup>-</sup>, using spectrometric techniques. Cations (Na, K, Ca, and Mg) and trace elements (arsenic (As), boron (B), barium (Ba), cadmium (Cd), cobalt (Co), cuprum (Cu), chromium (Cr), ferrum (Fe), manganese (Mn), molybdenum (Mo), nickel (Ni), lead (Pb), selenium (Se), silicium (Si), uranium (U), vanadium (V), tungsten (W), and zinc (Zn)) were analyzed using inductively coupled plasma mass spectroscopy (ICP-MS) at the ACME Analytical Laboratories in Canada.

The HPI, HEI, and  $C_d$  were calculated individually for each sampling location. These indices were mapped using ArcGIS software. The HPI provides an overall assessment of water quality with respect to heavy metal contamination.<sup>23</sup> It is calculated using equation 1<sup>24</sup>:

$$HPI = \sum WiQi / \sum Wi \quad (1)$$

here,  $Q_i$  shows the sub index of the  $i$ -th parameter,  $W_i$  shows the unit weight of the  $i$ -th parameter and  $i$ -th shows the number of parameters considered. Also, the sub-index ( $Q_i$ ) of the parameter can be estimated via equation 2:

$$Q_i = \sum_{i=1}^n \frac{|M_i(-)I_i|}{S_i - I_i} \times 100 \quad (2)$$

here,  $M_i$ ,  $I_i$  and  $S_i$  indicate, respectively, the monitored heavy metal, ideal and standard values of the  $i$ th parameter. The subtract sign (-) indicates the numerical difference between the two values, ignoring the algebraic sign.<sup>25</sup> The critical pollution index value is 100.<sup>26</sup>

HEI gives information about water quality according to the contents of heavy metals in water samples<sup>27</sup> and is expressed as equation 3:

$$HEI = \sum_{i=1}^n \frac{H_c}{H_{mac}} \quad (3)$$

here,  $H_c$  and  $H_{mac}$  present the monitored value and maximum admissible concentration (MAC) of the  $i$ -th parameter, respectively.<sup>27,28</sup> Furthermore, the  $C_d$  summarizes the merged effects of different water quality parameters deemed harmful for domestic use,<sup>29</sup> as estimated in equations 4 and 5:

$$C_d = \sum_{i=1}^n C_{f_i} \quad (4)$$

$$C_{f_i} = \frac{C_{A_i}}{C_{N_i}} - 1 \quad (5)$$

here,  $C_{f_i}$  = the contamination factor for the  $i$ -th component.  $C_{A_i}$  = analytical value for the  $i$ th component.  $C_{N_i}$  = upper permissible concentration of the  $i$ -th component and  $N$  denotes the normative value.

Multivariate statistical analysis methods were employed in this study. Groundwater quality data from the samples were analyzed using PASW (SPSS) 18.0 software. A correlation matrix (CM), based on Pearson's correlation coefficient, was used to examine the relationships between elements. principal component analysis (PCA) was employed to identify the primary factors (chemical data) linked to various natural and anthropogenic processes, as well as to pinpoint potential sources of heavy metals. Cluster analysis (CA) was performed to explore the associations between pollutant sources and different water quality parameters.

## Results and Discussion

HPI,  $C_d$ , and HEI were applied to evaluate pollution sources and heavy metal concentrations in the Jovein aquifer. The results revealed that the contents of Cr and As surpassed the maximum permissible limits recommended by the World Health Organization (WHO).<sup>30</sup> Statistical analyses of physicochemical parameters, metal concentrations, and

field measurements for the 22 groundwater samples are provided in Table 1.

Groundwater sampling from existing wells revealed that the groundwater in the Jovein aquifer is weakly alkaline. Electrical conductivity (EC) varied significantly, ranging from 354 to 2180  $\mu\text{S}/\text{cm}$ , with an average of 833.5  $\mu\text{S}/\text{cm}$ . The wide variation in EC values, along with total dissolved solids (TDS) levels ranging from 223 to 1373 mg/L, suggests heterogeneous hydrochemical processes in the study area.<sup>31</sup> The highest EC value (2180  $\mu\text{S}/\text{cm}$ ) was recorded near Kal Shur, indicating that river water intrusion with high salinity may be influencing groundwater chemistry in this region.

DO levels ranged from 6.7 to 11.7 mg/L, with a mean of 8 mg/L and a standard deviation of 1.4, indicating oxidizing groundwater conditions.

Heavy metal concentrations were analyzed to evaluate the processes controlling groundwater chemistry through interactions with serpentinites and the ophiolite complex. Although the concentrations of cations varied significantly, the dominant elements were B, followed by Cr, Ba, V, As, Na, and Mg, respectively.

The mean concentrations of trace elements in groundwater samples followed this order:

**Table 1.** Summarized statistics of selected physico-chemical parameters and chemical constituents in the area studied

| Parameter                    | Units                   | Max.  | Min. | Median | SD     | Mac      | Mean   |
|------------------------------|-------------------------|-------|------|--------|--------|----------|--------|
| EC                           | $\mu\text{S}/\text{cm}$ | 2180  | 354  | 704.5  | 437.84 | 1400b    | 833.55 |
| pH                           |                         | 8.6   | 7.2  | 8.3    | 0.3935 | 6.5-8.5a | 8.1364 |
| TDS                          | mg/L                    | 1373  | 223  | 443.8  | 275.8  | 1500     | 525    |
| DO                           | mg/L                    | 11.7  | 6.7  | 8      | 1.4    | -        | 8.6    |
| $\text{HCO}_3 + \text{CO}_3$ | mg/L                    | 244   | 61   | 152    | 48.4   | -        | 159.6  |
| Cl                           | mg/L                    | 3018  | 36   | 142    | 864    | 600      | 575.4  |
| $\text{SO}_4$                | mg/L                    | 1296  | 48   | 144    | 355    | 400      | 301.4  |
| Ca                           | mg/L                    | 360   | 0    | 20     | 164.4  | 200      | 73.6   |
| K                            | mg/L                    | 351   | 0    | 0      | 78.2   | 29.6     | 0.02   |
| Mg                           | mg/L                    | 432   | 12   | 24     | 108.8  | 150      | 70.6   |
| Na                           | mg/L                    | 1380  | 46   | 161    | 363.5  | 200      | 334.9  |
| Al                           | ppb                     | 14    | 1    | 3      | 3.4    | 200      | 4.04   |
| As                           | ppb                     | 10.5  | 0    | 4.4    | 3      | 10       | 4.3    |
| B                            | ppb                     | 1475  | 30   | 148.5  | 289.7  | 300      | 218.5  |
| Ba                           | ppb                     | 63.7  | 4.5  | 17.3   | 17.6   | 700      | 23.9   |
| Cr                           | ppb                     | 122.9 | 12   | 37.2   | 29.5   | 50       | 44.5   |
| Cu                           | ppb                     | 3.1   | 0.3  | 1.05   | 0.7    | 1000     | 1.25   |
| Li                           | ppb                     | 22.2  | 1    | 2.5    | 4      | n.a      | 3.7    |
| Mo                           | ppb                     | 5.5   | 0.5  | 2.5    | 1.5    | 40       | 2.6    |
| Sb                           | ppb                     | 0.11  | 0    | 0      | 0.04   | 5        | 0.03   |
| Se                           | ppb                     | 13.2  | 0.8  | 2.5    | 2.6    | 10       | 2.9    |
| U                            | ppb                     | 6.01  | 0    | 0.13   | 1.4    | 2        | 0.6    |
| V                            | ppb                     | 54.6  | 0.9  | 10.4   | 15.7   | n.a      | 16.1   |
| W                            | ppb                     | 0.14  | 0    | 0.04   | 0.03   | n.a      | 0.06   |
| Zn                           | ppb                     | 12.7  | 0    | 0.55   | 2.7    | 5000     | 1.2    |

MAC, maximum allowable concentration<sup>30-32</sup> (n.a: not available).

B > Cr > Ba > V > As > Al > Li > Se > Mo > Cu > Zn > U > W > Sb (Figure S2). The concentrations of all measured metals were below their respective MAC values. Figure 1 illustrates the relationship between pH and total metal concentrations (mg/L). Based on this analysis, all samples were within a near-neutral, low-metal zone, consistent with findings reported by Selvam.<sup>32</sup>

Metal contamination is widely recognized as being exacerbated by human activities and various chemical industries.<sup>33</sup> The ratio of pH to the sum of trace elements showed that 95% of the samples were within the low-pollution zone, while the remaining 5% fell into the medium-pollution category. These results suggest that the groundwater in the Jovein aquifer is not contaminated with heavy metals.<sup>26</sup>

Table 2 and Figure 2 indicate the observations of the pollution evaluation indices. HPI was calculated individually for each sampling point based on international standards.<sup>27</sup> The range and mean value of HPI were found to be 57.14–91.74 and 81.48, respectively. The index values (Figure 2) revealed that, for all samples, the HPI was below the critical pollution index (<100) for drinking water. This indicates that while the HPI of the groundwater was below the critical threshold, the levels were relatively high, with a mean value of 81.48.  $C_d$  was used as a reference to estimate the extent of metal pollution<sup>34</sup> in relation to background levels.<sup>35</sup> The range and mean values of  $C_d$  were 0.10–10.43 and 8.23, respectively. The  $C_d$  values are classified into three categories<sup>27,29</sup>: low ( $C_d < 1$ ), medium ( $C_d = 1-3$ ), and high ( $C_d > 3$ ). Based on the current study, 96% of the samples fell within the highly polluted category ( $C_d > 3$ ). Moreover, Edet and Offiong<sup>27</sup> proposed the HEI to classify samples into three categories based on heavy metal content: low (HEI < 10), medium (HEI = 10–20), and high (HEI > 20). Based on the HEI findings, over 95% of the samples were categorized as having low contamination with regard to heavy metals.

PCA was applied to further investigate metal pollution

Table 2. Indices of groundwater pollution in the region studied

|       | Mean  | Min   | Max   |
|-------|-------|-------|-------|
| HEI   | 2.44  | 0.57  | 10.06 |
| HPI   | 81.48 | 57.14 | 91.74 |
| $C_d$ | 8.23  | 0.1   | 10.3  |

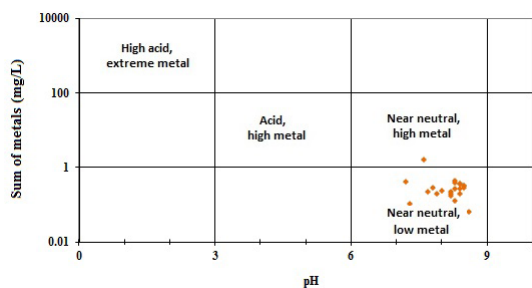


Figure 1. Classification of the Water Samples According to the Plot of Elemental Load and pH<sup>33</sup>

and identify potential sources.<sup>36</sup> Table 3 summarizes the calculated factor loadings, cumulative percentages, and variances, revealing five factors that collectively explain 86.57% of the total variance. According to the Kaiser criterion,<sup>37</sup> only factors with eigenvalues  $\geq 1$  are considered significant sources of variance, with priority given to factors with the highest eigenvector sums. Five factors were extracted from the groundwater data, each with eigenvalues greater than 1. Kaiser-Meyer-Olkin (KMO) and Bartlett's tests of sphericity were performed to assess the suitability of the dataset for PCA, as shown in Table 4. The results—KMO=0.51 and Bartlett's test  $\chi^2=332.29$  (df=120,  $P < 0.001$ )—indicated that factor analysis (FA) was effective for reducing dimensionality.<sup>38</sup>

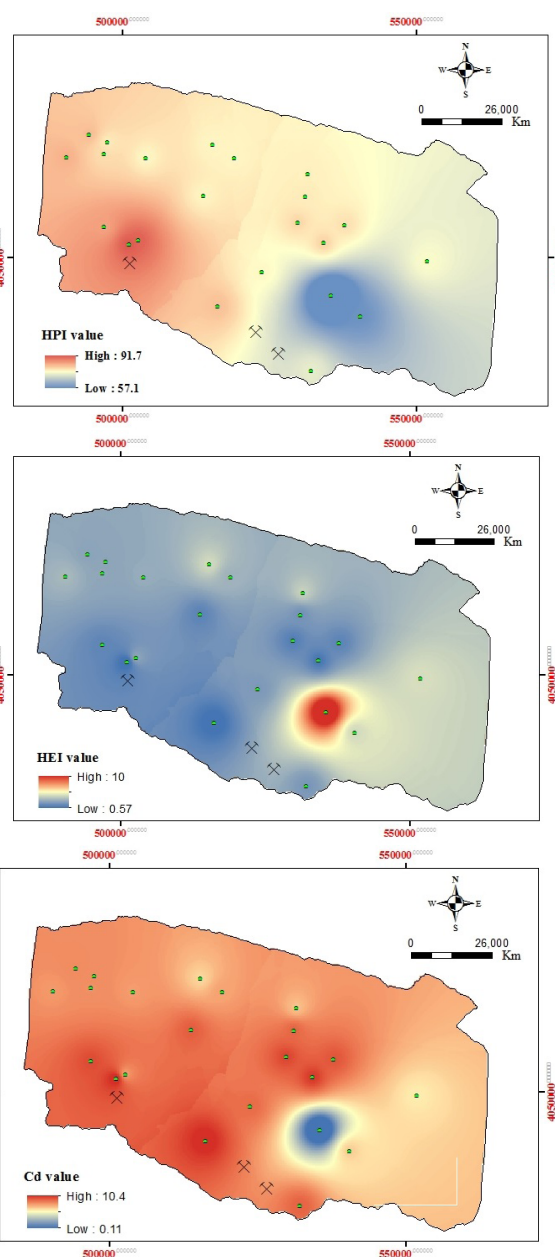


Figure 2. Variation of the Groundwater Indices Values (HPI, HEI,  $C_d$ ) in the Area Studied

Positive PCA scores indicated that the water samples were strongly influenced by parameters that were significantly loaded onto a specific factor, while negative scores suggested a minimal influence from those parameters.<sup>33</sup> Five independent factors were extracted. The combined contribution of PC1 and PC2 accounted for 62.37% of the dataset's variability (Figure 3), highlighting their significant role in influencing groundwater chemical evolution.

**Table 3.** Factor Loading for the Selected Physicochemical Variables in the Area Studied

|               | PC1         | PC2         | PC3         | PC4         | PC5         |
|---------------|-------------|-------------|-------------|-------------|-------------|
| Al            | 0.00        | 0.20        | -0.45       | <b>0.82</b> | 0.11        |
| As            | <b>0.81</b> | 0.44        | -0.01       | -0.01       | 0.11        |
| B             | <b>0.86</b> | -0.31       | -0.12       | -0.30       | -0.06       |
| Ba            | 0.26        | -0.33       | <b>0.76</b> | 0.21        | -0.30       |
| Cr            | 0.22        | <b>0.80</b> | 0.19        | 0.18        | 0.08        |
| Cu            | <b>0.87</b> | -0.03       | -0.31       | 0.14        | 0.11        |
| Mo            | <b>0.81</b> | 0.42        | -0.20       | 0.11        | 0.04        |
| Sb            | <b>0.57</b> | -0.10       | <b>0.55</b> | 0.42        | 0.17        |
| Se            | <b>0.86</b> | -0.27       | -0.19       | -0.24       | -0.15       |
| U             | <b>0.84</b> | -0.43       | 0.02        | -0.19       | 0.00        |
| V             | <b>0.68</b> | <b>0.54</b> | 0.13        | -0.16       | 0.21        |
| W             | 0.22        | <b>0.80</b> | 0.34        | -0.11       | 0.19        |
| Zn            | -0.27       | -0.47       | -0.01       | -0.11       | <b>0.75</b> |
| EC            | <b>0.82</b> | -0.33       | -0.08       | 0.17        | -0.17       |
| pH            | -0.23       | <b>0.77</b> | -0.18       | -0.03       | -0.44       |
| DO            | -0.08       | <b>0.76</b> | 0.01        | -0.35       | 0.10        |
| Eigen values  | 6.02        | 3.96        | 1.48        | 1.34        | 1.06        |
| % of variance | 37.61       | 24.76       | 9.23        | 8.35        | 6.62        |
| Cumulative %  | 37.61       | 62.37       | 71.60       | 79.95       | 86.57       |

Bold numbers: Values which are greater than 0.5, was effective parameter in the factor analysis.

**Table 4.** Pearson Correlation Coefficient Between Variables in Groundwater Samples

|    | Al    | As          | B           | Ba          | Cr          | Cu          | Mo          | Sb          | Se          | U           | V           | W           | Zn    | EC    | pH          | DO   |
|----|-------|-------------|-------------|-------------|-------------|-------------|-------------|-------------|-------------|-------------|-------------|-------------|-------|-------|-------------|------|
| Al | 1.00  |             |             |             |             |             |             |             |             |             |             |             |       |       |             |      |
| As | 0.10  | 1.00        |             |             |             |             |             |             |             |             |             |             |       |       |             |      |
| B  | -0.21 | <b>0.54</b> | 1.00        |             |             |             |             |             |             |             |             |             |       |       |             |      |
| Ba | -0.27 | -0.02       | 0.21        | 1.00        |             |             |             |             |             |             |             |             |       |       |             |      |
| Cr | 0.17  | 0.41        | -0.14       | 0.03        | 1.00        |             |             |             |             |             |             |             |       |       |             |      |
| Cu | 0.22  | <b>0.66</b> | <b>0.71</b> | 0.08        | 0.22        | 1.00        |             |             |             |             |             |             |       |       |             |      |
| Mo | 0.21  | <b>0.85</b> | <b>0.53</b> | -0.06       | <b>0.52</b> | <b>0.79</b> | 1.00        |             |             |             |             |             |       |       |             |      |
| Sb | 0.11  | <b>0.49</b> | 0.32        | <b>0.52</b> | 0.13        | 0.31        | 0.34        | 1.00        |             |             |             |             |       |       |             |      |
| Se | -0.15 | <b>0.55</b> | <b>0.95</b> | 0.19        | -0.10       | <b>0.75</b> | <b>0.57</b> | 0.28        | 1.00        |             |             |             |       |       |             |      |
| U  | -0.20 | <b>0.51</b> | <b>0.92</b> | 0.30        | -0.24       | <b>0.67</b> | 0.45        | <b>0.49</b> | <b>0.85</b> | 1.00        |             |             |       |       |             |      |
| V  | -0.03 | <b>0.86</b> | 0.43        | -0.05       | <b>0.50</b> | 0.43        | <b>0.74</b> | 0.42        | 0.42        | 0.40        | 1.00        |             |       |       |             |      |
| W  | -0.02 | <b>0.52</b> | -0.06       | 0.00        | <b>0.71</b> | 0.09        | 0.41        | 0.16        | -0.08       | -0.12       | <b>0.65</b> | 1.00        |       |       |             |      |
| Zn | -0.09 | -0.41       | -0.06       | -0.07       | -0.29       | -0.11       | -0.38       | -0.12       | -0.15       | -0.04       | -0.29       | -0.27       | 1.00  |       |             |      |
| EC | 0.07  | 0.40        | <b>0.79</b> | 0.40        | 0.06        | <b>0.84</b> | <b>0.56</b> | 0.43        | <b>0.77</b> | <b>0.78</b> | 0.21        | -0.16       | -0.16 | 1.00  |             |      |
| pH | 0.18  | 0.09        | -0.33       | -0.30       | <b>0.49</b> | -0.26       | 0.15        | -0.40       | -0.27       | -0.51       | 0.21        | 0.43        | -0.53 | -0.39 | 1.00        |      |
| DO | -0.11 | 0.23        | -0.21       | -0.36       | <b>0.59</b> | -0.06       | 0.17        | -0.22       | -0.23       | -0.31       | 0.30        | <b>0.62</b> | -0.25 | -0.28 | <b>0.48</b> | 1.00 |

Bold numbers: Values which are greater than 0.5, was effective parameter in the factor analysis.

Factor 1 (PC1): Contributed 37.61% of the total variance, with high loadings on EC (r=0.82), B (r=0.86), As (r=0.81), Sb (r=0.57), Se (r=0.86), Mo (r=0.81), Cu (r=0.87), U (r=0.84), and V (r=0.68). The sources of these elements, particularly EC, As, Sb, Se, Mo, Cu, and V, were linked to the leaching of massive sulfide veins, suggesting a geogenic origin. Maximum values were observed in samples W2, W3, W7, and W17.

Factor 2 (PC2): Accounted for 24.76% of the total variance, with high loadings on Cr (r=0.8), V (r=0.54), and W (r=0.8). These results reflect the effects of water-rock interaction with mafic and ultramafic rocks (ophiolite complex), chromite mining, and Joghatay ferrochromium factory activities, indicating both geogenic and anthropogenic sources. Significant values were found in samples W6, W16, W11, W12, and W17.

Factor 3 (PC3): Contributed 9.23% of the total variance, with high loadings on Ba (r=0.76) and Sb (r=0.55). These elements were influenced by leaching from massive sulfide veins, suggesting a geogenic origin. Samples W1, W2, W8, W11, and W16 were most affected.

Factor 4 (PC4): Accounted for 8.35% of the total

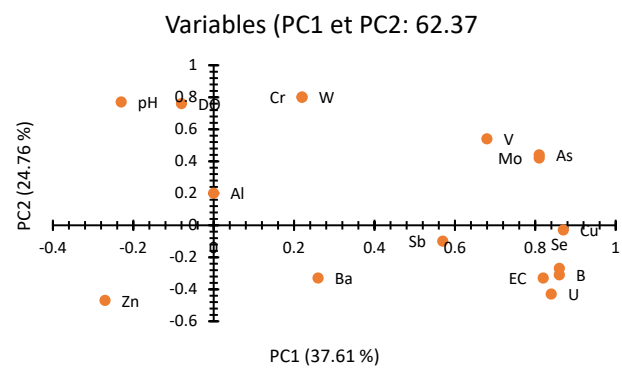


**Figure 3.** Ratio of Main PCA of the Groundwater Parameters

variance, with a high loading on Al ( $r=0.82$ ), likely controlled by the weathering of Al-silicate minerals. This factor, with a geogenic origin, was prominent in samples W7, W8, W15, W20, W21, and W22.

Factor 5 (PC5): Contributed 6.62% of the total variance, with a high loading on Zn ( $r=0.75$ ). The Zn concentrations, observed in samples W7, W14, W15, W16, and W17, were likely due to chromite mining and Joghatay ferrochromium activities, indicating anthropogenic sources.

R-mode CA grouped heavy metals into clusters based on variable similarities, while Q-mode analysis examined similarities between samples. Four main clusters (A, B, C, and D) were identified through dendrogram analysis (Figures 4a and 4b): Cluster A: Included B, Se, U, Cu, As, V, Mo, and EC. Cluster B: Contained Ba and Sb. Cluster C: Comprised Cr, W, DO, and pH. Cluster D: Included Zn.

The CA revealed the combined effects of natural hydrogeochemical processes and anthropogenic activities. The agreement between PCA and CA results suggests common sources and similar behavior of heavy metals during transport.

The CM was used to evaluate relationships between measured elements in groundwater samples (Table 4), providing insights into shared sources or influencing factors.<sup>39</sup> The CM showed significant correlations between, As, Mo, V, and Cu. Positive correlations between DO, pH, and elements such as As, Cr, V, W, and Mo were observed, while trace elements such as Cr, As, V, and Mo, which typically occur as soluble oxyanions in oxidizing waters,<sup>40</sup> contrasted with Mn, Co, and Ba, which exhibited higher concentrations in reducing environments.<sup>41</sup>

## Conclusion

Integrated pollution evaluation indices, CA, PCA, and CM were applied to study the influence of the ophiolite complex, hydrogeochemical characteristics, probable pollution sources, and processes affecting groundwater

chemistry in the Jovein aquifer. The results from CA, PCA, and pollution indices indicated that geogenic processes have a predominant influence on groundwater quality, while mining activities have a comparatively minor effect, limited primarily to Cr contamination in water sources. PCA results further revealed that Cr and Ni originate from the weathering and leaching of ultramafic and mafic rocks, as well as chromite mining activities in the area. Meanwhile, As and Cu were linked to sulfide mineralization, occurring in sulfide-bearing veinlets surrounded by altered host rock. In the area studied, key physicochemical parameters such as EC, pH, Ba, Na, K, Mn, Cu, Sb, and Se were within the permissible limits recommended by the WHO. However, concentrations of some heavy metals, including Cr, and metalloids such as As, exceeded these limits.  $C_d$  indicated that 96% of the samples were highly polluted ( $C_d > 3$ ). In contrast, HEI and HPI results for the samples were below critical levels. Nonetheless, most samples exhibited elemental concentrations near the threshold of critical values. Overall, the groundwater index suggests that the groundwater samples in the area studied present a low ecotoxicological risk concerning heavy metals.

## Acknowledgments

We thankfully appreciate the financial support from Department of Iranian environment, for their kind aid in sponsoring the project.

## Authors' Contribution

**Conceptualization:** Raheleh Hatefi, Morteza Razmara Farzagli.

**Data curation:** Raheleh Hatefi.

**Formal analysis:** Raheleh Hatefi, Morteza Razmara Farzagli.

**Funding acquisition:** Raheleh Hatefi.

**Investigation:** Raheleh Hatefi.

**Methodology:** Raheleh Hatefi.

**Project administration:** Raheleh Hatefi.

**Resources:** Raheleh Hatefi.

**Software:** Raheleh Hatefi.

**Supervision:** Raheleh Hatefi.

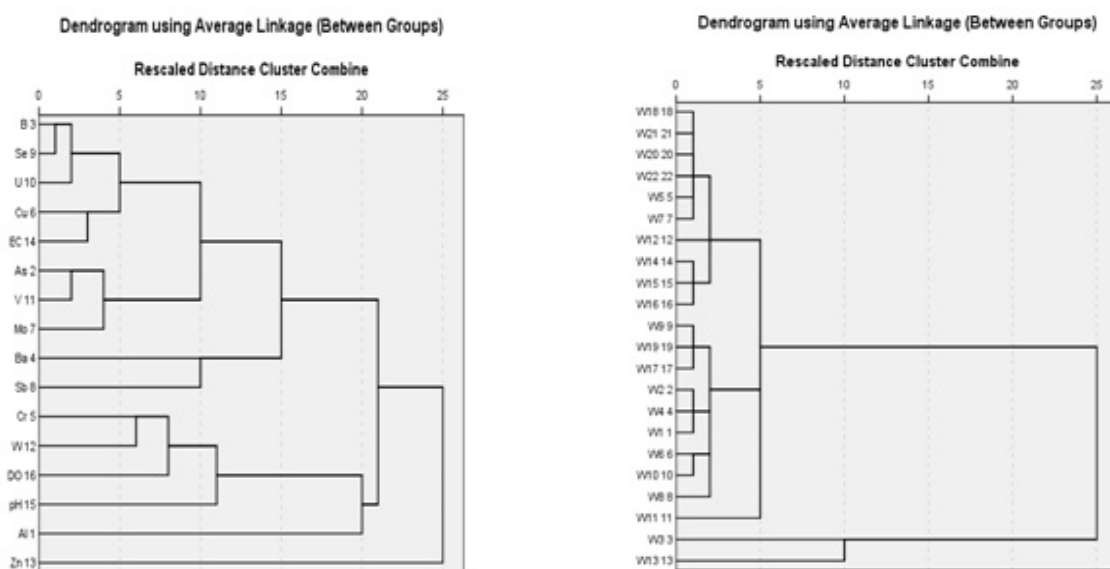


**Figure 4.** a) The Dendrogram presenting the clustering of 20 variables (in R-mode) in the area studied, b) The Dendrogram presenting the clustering of 20 variables (in Q-mode) in the area studied

**Validation:** Raheleh Hatefi.

**Visualization:** Raheleh Hatefi.

**Writing—original draft:** Raheleh Hatefi, Morteza Razmara Farzaghi.

**Writing—review & editing:** Seyed Mohammad Zamanzadeh.

### Competing Interests

The authors declare that they have no known competing financial interests or personal relationships that might have influenced the research presented in this paper.

### Ethical Approval

There were no ethical considerations to be considered in this research.

### Funding

Department of Iranian Environment supported this research financially.

### Supplementary File

Supplementary file 1 contains Figures S1-S2.

### References

1. Irunde R, Ijumulana J, Ligate F, Maity JP, Ahmad A, Mtamba J, et al. Arsenic in Africa: potential sources, spatial variability, and the state of the art for arsenic removal using locally available materials. *Groundw Sustain Dev*. 2022;18:100746. doi: [10.1016/j.gsd.2022.100746](https://doi.org/10.1016/j.gsd.2022.100746).
2. Rehman Nu, Ali W, Muhammad S, Tepe Y. Evaluation of drinking and irrigation water quality, and potential risks indices in the Dera Ismail Khan district, Pakistan. *Kuwait J Sci*. 2024;51(1):100150. doi: [10.1016/j.kjs.2023.11.001](https://doi.org/10.1016/j.kjs.2023.11.001).
3. Adimalla N, Wu J. Groundwater quality and associated health risks in a semi-arid region of south India: implication to sustainable groundwater management. *Hum Ecol Risk Assess*. 2019;25(1-2):191-216. doi: [10.1080/10807039.2018.1546550](https://doi.org/10.1080/10807039.2018.1546550).
4. He X, Li P, Wu J, Wei M, Ren X, Wang D. Poor groundwater quality and high potential health risks in the Datong basin, northern China: research from published data. *Environ Geochem Health*. 2021;43(2):791-812. doi: [10.1007/s10653-020-00520-7](https://doi.org/10.1007/s10653-020-00520-7).
5. Wu J, Zhang Y, Zhou H. Groundwater chemistry and groundwater quality index incorporating health risk weighting in Dingbian county, Ordos basin of northwest China. *Geochemistry*. 2020;80(4 Suppl):125607. doi: [10.1016/j.chemer.2020.125607](https://doi.org/10.1016/j.chemer.2020.125607).
6. Ahamad A, Janardhana Raju N, Madhav S, Gossel W, Ram P, Wycisk P. Potentially toxic elements in soil and road dust around Sonbhadra industrial region, Uttar Pradesh, India: source apportionment and health risk assessment. *Environ Res*. 2021;202:111685. doi: [10.1016/j.envres.2021.111685](https://doi.org/10.1016/j.envres.2021.111685).
7. Karimi A, Naghizadeh A, Biglari H, Peirovi R, Ghasemi A, Zarei A. Assessment of human health risks and pollution index for heavy metals in farmlands irrigated by effluents of stabilization ponds. *Environ Sci Pollut Res Int*. 2020;27(10):10317-27. doi: [10.1007/s11356-020-07642-6](https://doi.org/10.1007/s11356-020-07642-6).
8. Yadav A, Sonje A, Mathur P, Chandra A, Jain DA, Pardeshi C. Detailed study of ground water, contamination sources & approaches to clean ground water. *Pharmacie Globale*. 2012;3(2):1-5.
9. Mirzabeygi Rad Fard M, Yousefi M, Soleimani H, Mohammadi AA, Mahvi AH, Abbasnia A. The concentration data of fluoride and health risk assessment in drinking water in the Ardakan city of Yazd province, Iran. *Data Brief*. 2018;18:40-6. doi: [10.1016/j.dib.2018.02.069](https://doi.org/10.1016/j.dib.2018.02.069).
10. Subba Rao N, Ravindra B, Wu J. Geochemical and health risk evaluation of fluoride rich groundwater in Sattenapalle region, Guntur district, Andhra Pradesh, India. *Hum Ecol Risk Assess*. 2020;26(9):2316-48. doi: [10.1080/10807039.2020.1741338](https://doi.org/10.1080/10807039.2020.1741338).
11. Kanellopoulos C. Influence of ultramafic rocks and hot springs with travertine depositions on geochemical composition and baseline of soils. Application to eastern central Greece. *Geoderma*. 2020;380:114649. doi: [10.1016/j.geoderma.2020.114649](https://doi.org/10.1016/j.geoderma.2020.114649).
12. Nazari E, Razmara M. Evaluation of the heavy metal contaminations in water resources in ophiolitic complex of Pangi area, (Kadkan, NW Torbat Hydarieh, Iran). *J Middle East Appl Sci Technol*. 2014;6(2):152-6.
13. Tirkey P, Bhattacharya T, Chakraborty S. Water quality indices—important tools for water quality assessment: a review. *Int J Adv Chem*. 2013;1(1):15-28.
14. Singh PK, Verma P, Tiwari AK, Sharma S, Purty P. Review of various contamination index approaches to evaluate groundwater quality with geographic information system (GIS). *Int J ChemTech Res*. 2015;7(4):1920-9.
15. Li P, Karunanidhi D, Subramani T, Srinivasamoorthy K. Sources and consequences of groundwater contamination. *Arch Environ Contam Toxicol*. 2021;80(1):1-10. doi: [10.1007/s00244-020-00805-z](https://doi.org/10.1007/s00244-020-00805-z).
16. Brhane GK. Irrigation water quality index and GIS approach-based groundwater quality assessment and evaluation for irrigation purpose in Ganta Afshum Selected Kebeles, Northern Ethiopia. *Int J Emerg Trends Sci Technol*. 2016;3(9):4624-36. doi: [10.18535/ijetst/v3i09.10](https://doi.org/10.18535/ijetst/v3i09.10).
17. Bora M, Goswami DC. Water quality assessment in terms of water quality index (WQI): case study of the Kolong River, Assam, India. *Appl Water Sci*. 2017;7(6):3125-35. doi: [10.1007/s13201-016-0451-y](https://doi.org/10.1007/s13201-016-0451-y).
18. Bhuiyan MA, Parvez L, Islam MA, Dampare SB, Suzuki S. Heavy metal pollution of coal mine-affected agricultural soils in the northern part of Bangladesh. *J Hazard Mater*. 2010;173(1-3):384-92. doi: [10.1016/j.jhazmat.2009.08.085](https://doi.org/10.1016/j.jhazmat.2009.08.085).
19. Gad M, Gaagai A, Eid MH, Szűcs P, Hussein H, Elsherbiny O, et al. Groundwater quality and health risk assessment using indexing approaches, multivariate statistical analysis, artificial neural networks, and GIS techniques in El Kharga Oasis, Egypt. *Water*. 2023;15(6):1216. doi: [10.3390/w15061216](https://doi.org/10.3390/w15061216).
20. Shafaii Moghadam H, Zaki Khedr M, Arai S, Stern RJ, Ghorbani G, Tamura A, et al. Arc-related harzburgite–dunite–chromitite complexes in the mantle section of the Sabzevar ophiolite, Iran: a model for formation of podiform chromitites. *Gondwana Res*. 2015;27(2):575-93. doi: [10.1016/j.gr.2013.09.007](https://doi.org/10.1016/j.gr.2013.09.007).
21. Fantoni D, Brozzo G, Canepa M, Cipolli F, Marini L, Ottonello G, et al. Natural hexavalent chromium in groundwaters interacting with ophiolitic rocks. *Environ Geol*. 2002;42(8):871-82. doi: [10.1007/s00254-002-0605-0](https://doi.org/10.1007/s00254-002-0605-0).
22. Margiotta S, Mongelli G, Summa V, Paternoster M, Fiore S. Trace element distribution and Cr(VI) speciation in Ca-HCO<sub>3</sub> and Mg-HCO<sub>3</sub> spring waters from the northern sector of the Pollino massif, southern Italy. *J Geochem Explor*. 2012;115:1-12. doi: [10.1016/j.gexplo.2012.01.006](https://doi.org/10.1016/j.gexplo.2012.01.006).
23. Uugwanga MN, Kgabi NA. Heavy metal pollution index of surface and groundwater from around an abandoned mine site, Klein Aub. *Phys Chem Earth, Parts*. 2021;124(Pt 1):103067. doi: [10.1016/j.pce.2021.103067](https://doi.org/10.1016/j.pce.2021.103067).
24. Mohan SV, Nithila P, Reddy SJ. Estimation of heavy metals in drinking water and development of heavy metal pollution index. *J Environ Sci Health A Environ Sci Eng Toxicol*. 1996;31(2):283-9. doi: [10.1080/10934529609376357](https://doi.org/10.1080/10934529609376357).
25. Prasad B, Mondal KK. The impact of filling an abandoned open cast mine with fly ash on ground water quality: a case study. *Mine Water Environ*. 2008;27(1):40-5. doi: [10.1007/s10230-007-0021-5](https://doi.org/10.1007/s10230-007-0021-5).
26. Moldovan A, Török AI, Kovacs E, Cadar O, Mirea IC, Micle V. Metal contents and pollution indices assessment of surface water, soil, and sediment from the Arieş River basin mining

- area, Romania. *Sustainability*. 2022;14(13):8024. doi: [10.3390/su14138024](https://doi.org/10.3390/su14138024).
27. Edet AE, Offiong OE. Evaluation of water quality pollution indices for heavy metal contamination monitoring. A study case from Akpabuyo-Odukpani area, Lower Cross River basin (southeastern Nigeria). *GeoJournal*. 2002;57(4):295-304. doi: [10.1023/B:GEJO.0000007250.92458.de](https://doi.org/10.1023/B:GEJO.0000007250.92458.de).
  28. Hosseinpour Moghaddam M, Lashkaripour GR, Dehghan P. Assessing the effect of heavy metal concentrations (Fe, Pb, Zn, Ni, Cd, As, Cu, Cr) on the quality of adjacent groundwater resources of Khorasan steel complex. *Int J Plant Anim Environ Sci*. 2014;4(2):511-8.
  29. Backman B, Bodiš D, Lahermo P, Rapant S, Tarvainen T. Application of a groundwater contamination index in Finland and Slovakia. *Environ Geol*. 1998;36(1):55-64. doi: [10.1007/s002540050320](https://doi.org/10.1007/s002540050320).
  30. World Health Organization (WHO). *Guidelines for Drinking-Water Quality*. 3rd ed. WHO; 2004.
  31. Siegel FR. *Environmental Geochemistry of Potentially Toxic Metals*. Berlin: Springer; 2002.
  32. World Health Organization (WHO). *Guidelines for Drinking-Water Quality: Recommendations*. Geneva, Switzerland: WHO; 1993.
  33. Prasanna MV, Chidambaram S, Shahul Hameed A, Srinivasamoorthy K. Study of evaluation of groundwater in Gadilam basin using hydrogeochemical and isotope data. *Environ Monit Assess*. 2010;168(1-4):63-90. doi: [10.1007/s10661-009-1092-5](https://doi.org/10.1007/s10661-009-1092-5).
  34. Al-Ami MY, Al-Nakib SM, Ritha NM, Nouri AM, Al-Assina A. Water quality index applied to the classification and zoning of Al-Jaysh canal, Baghdad-Iraq. *J Environ Sci Health A Environ Sci Eng Toxicol*. 1987;22(4):305-19. doi: [10.1080/10934528709375351](https://doi.org/10.1080/10934528709375351).
  35. Varol M. Assessment of heavy metal contamination in sediments of the Tigris River (Turkey) using pollution indices and multivariate statistical techniques. *J Hazard Mater*. 2011;195:355-64. doi: [10.1016/j.jhazmat.2011.08.051](https://doi.org/10.1016/j.jhazmat.2011.08.051).
  36. Liu J, Kang H, Tao W, Li H, He D, Ma L, et al. A spatial distribution - principal component analysis (SD-PCA) model to assess pollution of heavy metals in soil. *Sci Total Environ*. 2023;859(Pt 1):160112. doi: [10.1016/j.scitotenv.2022.160112](https://doi.org/10.1016/j.scitotenv.2022.160112).
  37. Kaiser HF. The application of electronic computers to factor analysis. *Educ Psychol Meas*. 1960;20(1):141-51. doi: [10.1177/001316446002000116](https://doi.org/10.1177/001316446002000116).
  38. Zhou F, Huang GH, Guo H, Zhang W, Hao Z. Spatio-temporal patterns and source apportionment of coastal water pollution in eastern Hong Kong. *Water Res*. 2007;41(15):3429-39. doi: [10.1016/j.watres.2007.04.022](https://doi.org/10.1016/j.watres.2007.04.022).
  39. Shi W, Li T, Feng Y, Su H, Yang Q. Source apportionment and risk assessment for available occurrence forms of heavy metals in Dongdahe Wetland sediments, southwest of China. *Sci Total Environ*. 2022;815:152837. doi: [10.1016/j.scitotenv.2021.152837](https://doi.org/10.1016/j.scitotenv.2021.152837).
  40. Izbicki JA, Ball JW, Bullen TD, Sutley SJ. Chromium, chromium isotopes and selected trace elements, western Mojave Desert, USA. *Appl Geochem*. 2008;23(5):1325-52. doi: [10.1016/j.apgeochem.2007.11.015](https://doi.org/10.1016/j.apgeochem.2007.11.015).
  41. Chen K, Jiao JJ, Huang J, Huang R. Multivariate statistical evaluation of trace elements in groundwater in a coastal area in Shenzhen, China. *Environ Pollut*. 2007;147(3):771-80. doi: [10.1016/j.envpol.2006.09.002](https://doi.org/10.1016/j.envpol.2006.09.002).